Available online at www.sciencedirect.com
ScienceDirect
Procedia Materials Science 5 (2014) 622 – 629
Procedia Materials Science
www.elsevier.com/locate/procedia

International Conference on Advances in Manufacturing and Materials Engineering, AMME 2014

Investigation of HVOF Thermal sprayed Cr_3C_2-NiCr Cermet Carbide Coatings on Erosive Performance of AISI 316 Molybdenum steel

Manjunatha M[a], R S Kulkarni [a*], M Krishna[b]

[a] *Research scholar, Dept.of Mech. Engg., RV College of Engineering,Bangalore, India.*
[a*] *Professor and Head, Dept. of Mech. Engg., RV College of Engineering,Bangalore, India.*
[b] *Dean, R and D, Dept. of Mech. Engg., RV College of Engineering,Bangalore, India.*

Abstract

The objective of the work was to determine the effect of Cr_3C_2-NiCr coatings on erosive performance of AISI 316 molybdenum steel using Air Jet Erosion Tester. The coating of high velocity oxygen fuel (HVOF) thermal sprayed consisted of determining the differences in the composition mechanism. The coated samples were characterised by micro Vickers hardness and XRD. Erosion test were conducted with alumina particle of size 22-24 µm at temperature of 650 °C at impact angles 60°, 75° and 90°.The surface morphology of eroded higher impact angle (75°) specimen was examined by scanning electron microscopy (SEM). On the basis of microstructural and experimental results of the particle mass effect on the compared three compositions smaller weight losses and erosion rates under all the selected working conditions, which account for their higher erosion resistances.

Selection and peer-review under responsibility of Organizing Committee of AMME 2014

Keywords: Cr_3C_2-NiCr coatings; HVOF thermal spray; erosion

1. Introduction

Cermet carbide composite coatings, involving such ceramic particles embedded in a metallic matrix can be used to provide high erosive resistance to metal substrates [Baik K H (2006)]. WC and Cr_3C_2 carbides are refractory compounds that combine many favourable properties such as high hardness, certain plasticity and good wettability with the bonding metal [Barbezat G Nicoll A R et al (1993)].This advantageous combination can make these materials promising candidates as constituents of a protective coating with enhanced resistance against erosion, corrosion and mechanical wear [Chen J H et al (2009)].

* Corresponding author. Tel.: +91 99456 02861; fax: +91 80 2860 0337.
E-mail address: ravindraskulkarni@rvce.edu.in

Selection and peer-review under responsibility of Organizing Committee of AMME 2014
doi:10.1016/j.mspro.2014.07.308

Thermally sprayed coatings are widely used in various applications to combat various surface degradation processes such as wear, erosion, corrosion, etc. Air craft, textile, automobile and mining are some of the areas where thermally sprayed coatings are extensively used for various advantages that this class of coating offers. The high velocity oxy-fuel (HVOF) processes minimise decomposition of the carbide phase due to lower heat enthalpy and shorter duration involved in the coating processes [Barbezat G et al (1993)]. In addition, higher particle velocity during deposition provides several advantages such as lower porosity, higher bond strength and hardness.

Chromium carbides are used as abrasive, Cr_3C_2 being harder than steel but softer than tungsten carbides. Chromium carbide is an extremely hard refractory ceramic material and demonstrates excellent strength, anti-erosion and corrosion properties, permanent non magnetizability and surface illustriousness [Benesovsky F et al (1953)].It has the appearance of a gray powder with orthorhombic crystal structure. Despite chromium carbide's excellent wear- and corrosion-resistant properties, it is not used as primary carbide in industry owing to its lower hardness and normal temperature (550 °C) in comparison to other carbides (such as tungsten carbide) [Guo Q et al (2002)]. Several attempts have been made to improve the hardness and wear property of chromium carbide coatings by varying the coating techniques, processing parameters and characteristics of the feedstock powder [Murthy JKN and Venkataraman B (2006)]. So Chromium carbide is used in combination with Ni-Cr, which improves the toughness and ductility of the coating [Murthy JKN and Bysakh S et al (2007)]. Ni-Cr alloy is generally used as metallic binder for providing good corrosion wear protection at high temperature [Ji G-C, et al (2006)]. These types of coatings are called "Cr_3C_2-NiCr coatings".

However, the effect of erosion performance of the coating is rarely investigated. The objective of the work was to determine the effect of Cr_3C_2-NiCr coatings on erosive performance of AISI 316 molybdenum steel using hot Air Jet Erosion Tester and characterise the microstructural changes.

2. Experimental procedure

2.1. Materials

Commercially available AISI 316 austenitic stainless steel plates have been chosen as the substrate material and they are cut into pieces of desired sizes, rectangular plates (75 mm × 25 mm ×5 mm in size) were used for erosion and hardness testing. Presence of chromium in stainless steel makes it corrosion resistant [Harvey (1979)]. Any stainless steel that contains more proportion of molybdenum content is called as molybdenum steel. Chemical composition is given in Table 1.

Table 1: Chemical composition of different elements present in the AISI 316 substrate material (wt %)

GRADE		C	Mn	Si	P	S	Cr	Mo	Ni	N
316	MIN	–	–	–	–	–	16.0	2.00	10.0	-
	MAX	0.08	2.0	1.00	0.045	0.03	18.0	3.00	14.0	0.10

Select compositions of coating material: Cr_3C_2–NiCr is very important to be very careful in selecting appropriate proportions coating system as well as correct composition of coating material. Improper selection again will lead to premature failure. Hence it becomes very important to select a proper coating composition as the requirement changes with different types of surface problems. Experiments carried by researchers have shown that Chromium carbide with nickel-chrome metal binder in different proportions coating done by using different methods of thermal spray process [Mohanty M (1996) and Kamal S et al (2008)].

Blending of powder: The first step in the forming of powder chromium carbide is the mixing or blending with Nickel chrome in required percentage increments up to 100 % (as shown Table 2). The Nickel chrome powder size was similar to the chromium carbide powder. In this work, three compositions of Cr_3C_2-NiCr powder (type: Amdry 5260, Japan) were selected and composition are given in Table 2.

Table 2: The 3 different powder chemical compositions of Chromium carbide-Nickel chrome

Coating	Nominal Composition	Powder type	Powder size Range (μm)	Hardness $HV_{0.1kg}$
A	Cr_3C_2-NiCr (85/15) %	Blend	11-44 μm	621.33
B	Cr_3C_2-NiCr (90/10) %	Blend	11-44 μm	875.33
C	Cr_3C_2-NiCr (95/5) %	Blend	11-44 μm	1065

2.2. *Coating Technique (HVOF Spray process)*

The HVOF spray technology can deposit a wide array of materials namely metals, ceramics and polymers. These coating can be deposited at high deposition rates with little substrate preparation and post-spray distortion. In this investigation, coating depositions were carried out using an 80 kW HVOF spray system (Model: Sulzer-Metco Diamond Jet 80 kW, Japan) at Spray met Technologies, Bangalore. The specimens were grit blasted at a pressure of 3 kg/cm^2 using alumina grits having a grit size of 60. The parameters listed in Table 3. The grit blasted specimens were cleaned with acetone in an ultrasonic cleaning unit. Spraying was carried out immediately after cleaning. Fuel (kerosene, acetylene, propylene and hydrogen) and oxygen are fed into the chamber. Combustion produces a hot high pressure flame which is forced down a nozzle increasing its velocity. Powder is preferably fed axially into the combustion chamber under high pressure or fed through the side of nozzle where the pressure is lower. Due to higher velocity the bond-strength of the coatings are higher. The powder to be sprayed are often not melted but accelerated in a high temperature and high velocity gas stream causing the phase of the sprayed material to change from solid to plastic (semi-molten) form [Rastegar F and Richardson D E (1997)]. When these particles strike the prepared substrate, they solidify to form a very dense and low porosity coating. HVOF is best recommended for Carbide matrix coatings. Carbide coatings sprayed by HVOF renders good hardness, wear resistance and abrasion resistance characteristics [Sidhu.T.S (2006)].

Table 3: Operating parameters used in the experiment

Parameter	Operating Range
Operating Power (Kw)	80
Current (Amps)	300 - 500
Fuel gas (propane) Flow rate (l/min)	50
Oxygen Flow rate (l/min)	280
Powder feed rate (g/min)	11.7
Nozzle to substrate distance (Stand-off distance) (mm)	100

2.3. *Coating structural Characterisation*

2.3.1. *X-Ray Diffraction Studies*

The different phases present in the coatings is identify by using X-ray diffraction technique (Model: XRD-7000, SHIMADJU, Japan) at RVCE, Bangalore. The characteristic d-spacing of all possible values are taken from JCPDS cards and were compared with d-values obtained from XRD patterns to identify the various X-ray peaks and wavelengths obtained.

2.3.2. *X-Ray Mapping Studies*

X-ray mapping was investigated by using scanning electron microscope (Model: JSM-6480, LV SEM, USA) in IISc, Bangalore. X-ray mapping are used to examine the two-dimensional distribution of elements on a specimen surface. Functions available for two-dimensional data include simple image processing such as various arithmetic operations and smoothing, line profile display and analytical functions such as distance measurement. In X-ray mapping, we can identify the each elements composition in microstructure with the help of SEM.

2.3.3. Micro Hardness Measurement

The Hardness measurements were carried out using a Vickers micro hardness tester (Model: METATECH, Pune) in RVCE, Bangalore. Vickers hardness test is used for very hard materials and parts of small cross section. After metallographic preparation consisting in coated sample cutting using an abrasive saw with coolant, the samples are mounting in epoxy rings and in pre-polishing by using polishing machines or polishing using diamond slurries on an automatic polish system to enhance reproducibility. The polished small sliced coated samples in required dimensions (25 mm ×5 mm ×5 mm in size).

2.3.4. Erosion Studies

Erosion test was carried out using an Air Jet Erosion Tester (Model: TR470-600, DUCOM Bangalore make). This is used to test the erosion resistance of solid materials to a stream of gas containing abrasive particulate. The instrument can be configured to test as per ASTM G76 specifications. The erosion resistance was determined using an abrasive flux Silica particles or aluminium oxide used as the erodent (3kg) were fed by a particle feeder at a controlled rate into the mixing chamber where they entrained the dry high velocity air coming from the compressor.

Table 4: Parameters used in Erosion test

Parameters	Operating range
Particle velocity, V (m/s)	80
Temperature, T (°C)	650
Impact angle, α (◦)	60, 75 and 90
Erodent Silica or Alumina (g/min)	5
Test time, t in minutes	10
Erodent Loading, L (Kg)	3

The mixer is heated at high temperature. The particles further accelerated as they moved with the air stream through a chromium carbide converging nozzle (1.5mm dia) and then finally hit the sample kept fixed on the sample holder. Standoff distance of the object and nozzle is 10mm. The impact angle was varied by simply varying the orientation of the sample surface with respect to the impinging particles stream. The erosion test was carried out as follows. The sample was first cleaned in acetone using an ultrasonic cleaner, dried and then weighed using an electronic balance having a resolution of 0.01 mg. The sample was next fixed to the sample holder of the erosion rig and eroded with silica particles at the predetermined particle feed rate, impact velocity and impact angle for a period of about 10 min. The sample was then removed, cleaned in acetone and dried and weighed to determine the weight loss.

3. Results and discussion

3.1. Phase analysis

The X-ray diffraction pattern of the Cr_3C_2/NiCr (85/15) % sprayed coating is shown in Fig.1. A great peak characteristic of a substantial amount of elemental chromium (Cr) is observed on the coating. A highest peak shows presence of pure chromium Carbide. The different intensities of peaks Cr_3C_2 are present in the coating. Minor Cr_3Ni_2 or NiCr peaks can be observed. The Cr_3Ni_2 peaks are formed by NiCr binder, in the present coating, NiCr binder is likely to melt first and dissolve some chromium carbide to form a liquid phase (Cr_3Ni_2) which may be rich in the Cr and C. it may become supersaturated. This supersaturated melt may become amorphous or nanocrystalline upon rapid solidification during the deposition process. Also, a very small amount of Cr_2O_3 was detected in HVOF coating whose relative peak intensity was less than 3%.It is to be noted that such oxide was present even in the powder. However, the relative peak intensity for Cr_2O_3 was slightly higher indicating the oxidation of molten particles and possibly some carbide particles occurred to a small extent during the HVOF process.

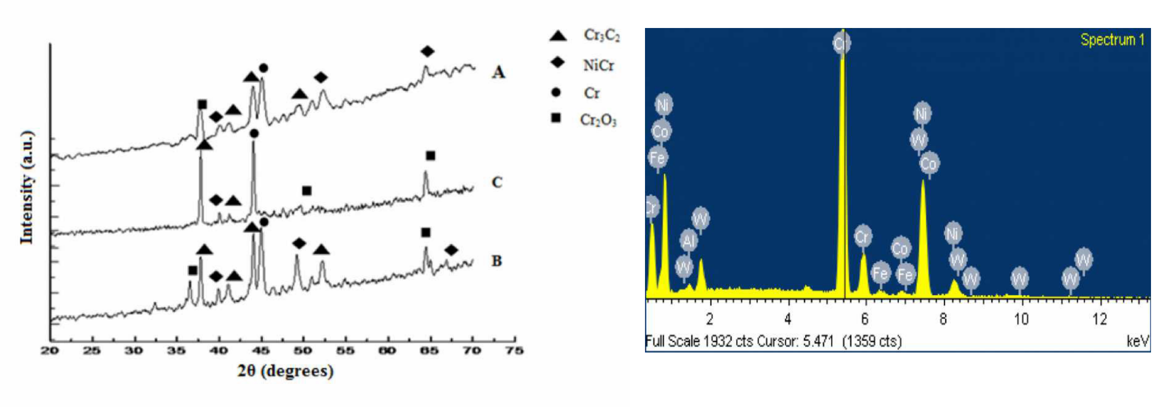

Fig.1.XRD patterns and profile mapping for Cr_3C_2/NiCr

The intensity of Cr_2O_3 peak is also found to increase heat treatment at 650 °C. A broad maximum peak in the range of 42 to 46 two theta (*2θ)* seems to indicate an amorphous phase in the deposit. Therefore, it is considered that nickel–chromium alloy and some Cr_3C_2 are melted and some amorphous phase forms. HVOF sprayed Cr_3C_2/NiCr (85/15) % coatings, exhibit an appreciable hardness due to Cr_3C_2, among other characteristics.

3.2. Erosion Wear Behaviour of Coatings

The erosion test was carried out at high temperature 650 °C at impact angles of 60°, 75° and 90° at a given gas fluid velocity using a high-temperature erosion tester. HVOF sprayed coatings Cr_3C_2-NiCr improve the erosion resistance of the substrate effectively. Coating Cr_3C_2-NiCr has good erosion resistance due to its high hardness and moderate toughness. Erosion wear is a systematic period, and every system parameter influences its behaviour. Among these parameters, the hardness and toughness of the target are the most important. A good erosion-resistant target must be tough and hard. The erosion tests were conducted to obtain two types of erosion data, namely the erosion mass loss and the erosion rates for the higher impact angles of samples A,B and C coatings listed in table 5.The erosion rate is defined as the ratio between the change in the sample mass and the mass of impacting particles. In each cycle the specimen was impacted by a preweighed increment of particle mass. After each particle-mass increment had impacted the sample, its surface was cleaned, the specimen was weighed and the change in specimen weight was recorded. The erosion rate for each successive particle increment was determined from the relation:

$$\text{Erosion rate (E r)} = \frac{\text{Change in mass of sample (weight loss)}}{\text{Mass of impacting particles}} \quad (1)$$

Where, Weight loss (w) = Initial weight- Final weight
The cumulative mass erosion tests were conducted only at the impact angles corresponding to maximum erosion.

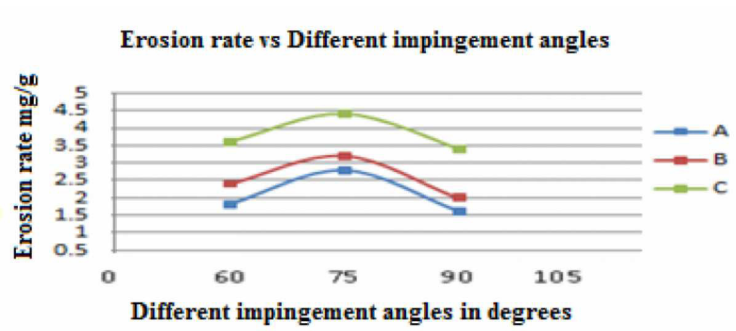

Fig.2. Comparison of Erosion Rate vs. Different Impingement angles for three Compositions of samples A, B and C

The aim of this work to study the only higher impact angle (75°), microstructures gives better results and suggests that the coating material behaves neither as purely ductile or nor purely brittle.

Table 5: Result of Erosion test for Higher impact angles 75° at a temperature of 650 °C, velocity 60m/sec and time kept constant (10 Min)

Coating	Higher Impact Angle α (degree)	Initial weight (w_1) g	Final weight (w_2) g	Weight Loss (w) g	Erosion rate (mg/g) ($\times 10^{-7}$)
A	75	29.244	29.23	0.014	2.8
B	75	23.859	23.843	0.016	3.2
C	75	23.858	23.836	0.022	4.4

From the Fig.2, graph observed that erosion rate is gradually increases with increase in impingement angle from 60°to 75° then it is decreases as impingement angle increases it is concluded that the erosion rate is maximum at impingement angle 75° and minimum at 90° impact angle. Erosion testing of the sprayed coatings found that decreasing the carbide content, and overall hard phase content (oxides and carbides), decreased the erosion rate for 90° impact. In addition, for 75° impact the erosion rate remained fairly constant regardless of carbide or hard phase content. The three compositions of coated samples, Cr_3C_2 -NiCr gives better results for both 60° and 75° than at 90° angle. In the both cases high erosion rate occur at 60° and 75°.

3.3. Micro Structural Characterization of Eroded Surfaces

3.3.1. Micrographs of Eroded sample A at 75° impingement of Cr_3C_2/NiCr (85/15) % Coating

Fig.3. (a), (b), (c) in the case of erosion, at higher impact angle, indentation impressions due to the impingement of erodent on the surface are clearly seen. In ductile erosion one of the common mechanisms is the material removal from the lips that are formed around the impact craters due to strain localization. Worn surface morphologies impact angle of Cr_3C_2/NiCr (85/15) % coating shows the chipping-type craters owing to the action of impacting particles. The impact craters were accompanied by much plastically deformed material around their rims. Removal of material apparently resulted from formation of protuberant deformed lips and their subsequent fracture by the impacting particles. By comparison, impact craters on worn surface of Cr_3C_2/NiCr (85/15) % composite coating are obviously smaller in size and depth than those of 60° impact angle, thereby improving the erosive resistance of the substrate.
Fine surface and subsurface small cracks occurred at the martensitic grains during high incident angle erosion, induced by the resolved normal stress. Cracking therefore was one of the major mechanisms involved in repetitious erosion fracturing for all tempering treatments. Short groove and smear craters from high incident angle erosion. The surface features of the centre of the smear crater are also dominated by grain ejection and some larger scaled flakes of deformed materials as seen in Fig.3 (a), (b), it is evident from the BSE image in Fig. (c) and (d) that these flakes consist primarily of deformed target chromium with traces of smeared erodent material in some regions. These angles induced random damaged marks (marked sky blue long arrow). For the two-phase material, the grain boundary provides the cracking site during erosion impact.

3.3.2. Micrographs of Eroded sample B at 75° impingement of Cr_3C_2/NiCr (90/10) % Coating

The micrographs of sample B, Fig.3 (e), (f), (g), (h) impact angle 75°of morphologies illustrates similar cracked and chipped morphology, indicating the same brittle erosion mechanism occurred. Erosion wastages occurred by large cracking and chipping mechanism of fractured and loosened pieces, the size of which is determined by the splat sizes of coatings. Cracking is thought to form first at “splat boundary” during impact of particles. Under continual impact of particles the radial and lateral cracks developed, then fractured and loosened pieces were chipped off. Finally, many small voids and pits formed. The effect of the impingement angle on the material removal mechanisms is clearly demonstrated. It is evident that at shallow impingement angles, erosion damage is dominated by both grain ejection and plastic deformation of the materials. Further, in the plastically deformed areas, grooves or plough marks are often observed. The plastic grooves, in many instances similar to scratches produced on chromium surfaces. However, the erosion cracks were observed for low impact angles (60° and 90°) the coating possessing the irregular weak structure displayed the highest erosion wastage.

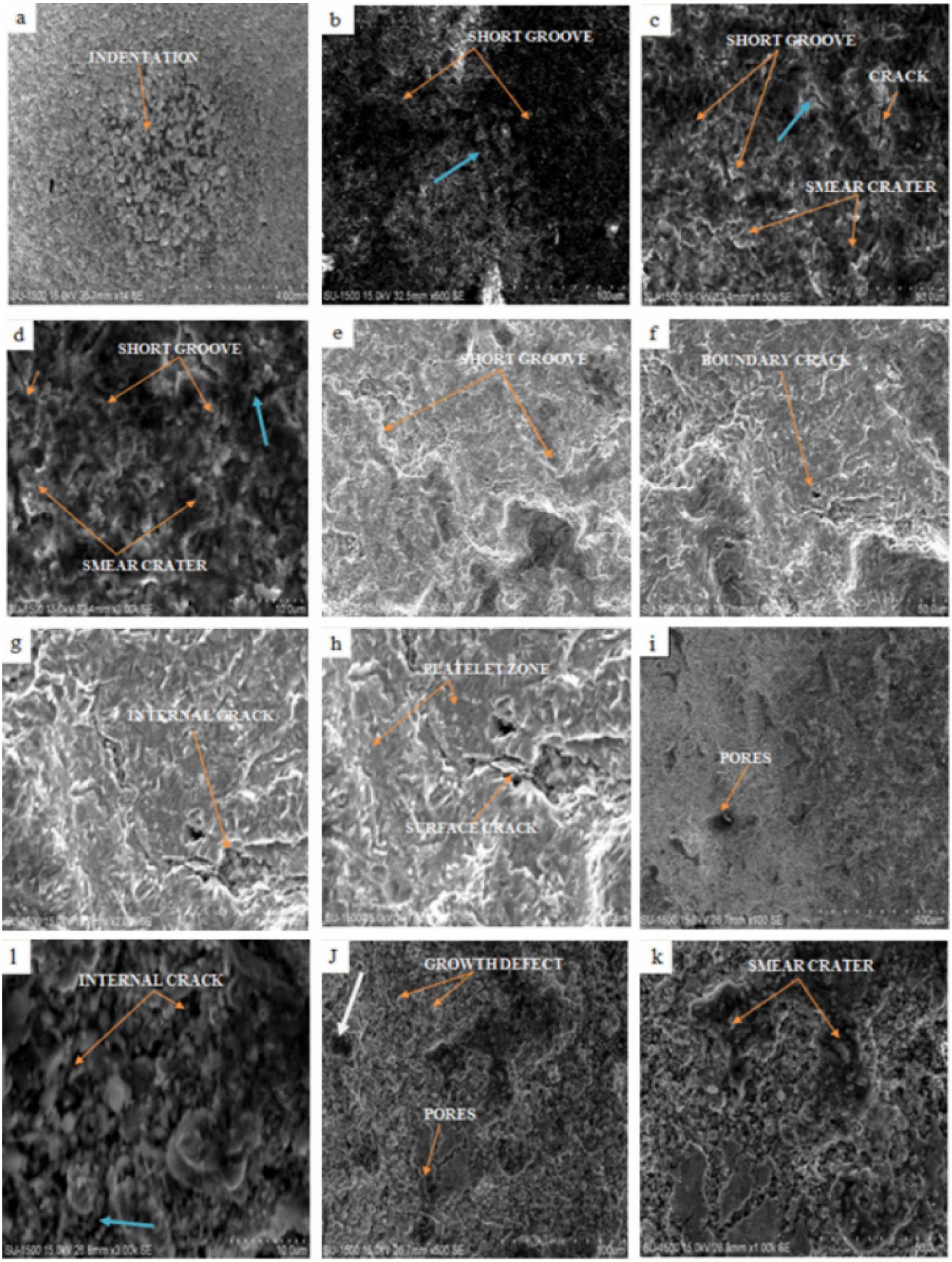

Fig.3. Micrographs of Eroded Cr_3C_2/NiCr coatings at 75° impingement: (1) Micrograph a, b, c and d for coating A ;(2) Micrograph e, f,g and h for coating B ;(3) Micrograph i,j,k and l for coating C.

3.3.3. Micrographs of Eroded sample C at 75° impingement of Cr_3C_2/NiCr (95/5) % Coating

The micrographs of sample C eroded impact surfaces shows the corresponding areas of the same materials eroded at samples B impact angles. Fig. 3 (i), (j), (k), (l) impact angle 75° of morphologies illustrates similar cracked and chipped morphology. Also, the eroded surfaces include more number of Cr_2O_3, different types of cracks and tiny pores. Some of the cracks extended from the surface to the subsurface, while others originated from the subsurface. These cracks became connected which caused the material to break down further. Fine surface and subsurface cracks occurred at the martensitic grains during high incident angle erosion, induced by the resolved normal stress.The sample C is oppositely to the sample A, the coating had the coarsest structure and weakest splat boundary which resulted in its highest erosion wastage and rough surface morphology.

4. Conclusions

We conclude in this our work; the erosion rate was decrease with increase in content of NiCr metallic binder and decrease in porosity of the coating by using HVOF method. A comparison of the morphological features on the eroded surfaces of the high-purity Cr_3C_2/NiCr (85/15) %, Sample subjected to low impact angles. 60° and 90° posses low erosion rate than sample B and C.

- HVOF sprayed Cr_3C_2/NiCr (85/15) % coatings offer excellent corrosion and oxidation resistance.
- From the graph observed that erosion rate is gradually increases with increase in impingement angle from 60° to 75° then it is decreases as impingement angle increases it is concluded that the erosion rate is maximum at impingement angle 75°and minimum at 90° impact angle.
- High temperature erosion resisting performance and durability of the HVOF sprayed coating were superior to the other kind of specimens examined.
- Prior heat treatment of Cr_3C_2/NiCr (85/15) % at 650 °C enhances the erosion resistance. The improvement in erosion is found to have strong dependence on impact angle.
- Similarly, erosion wear resistance also increased with increasing binder content NiCr added to the chromium coating. This behaviour can be easily predicted with the help of facto graph.

References

Baik K H, 2006: *Mater. Trans*.vol. 47, pp 2815–2820.

Barbezat G, Nicoll A R, A. Sickinger, 1993. Abrasion, erosion and scuffing resistance of carbide and oxide ceramic thermal sprayed coatings for different applications, *Wear,* vol. 162-164, pp 529–537.

Benesovsky F, Schwarzkopf P, Kieffer R, 2009. Refrctory hard metals: borides, carbides, nitrides and silicades. New York:1953.

Barbezat G, Karimi A, Verdon Ch, 1993. Microstructure and hydro abrasive wear behaviour of high velocity oxy-fuel thermally sprayed WC–Co (Cr) coatings, *surface coating Technology* vol. 57, pp 81–89.

Chen J H, Chen P N, Hua P H, Chang Y and W. Wu. *Mater. Trans.* vol. 50, pp 689–694.

Guo Q, Wang J, Sun B, Nishio M et a l, 2002. *Therm spray Technol*; vol. 11,pp 261

Harvey, 1979, Engineering properties of steel (Metals Park, Ohio: Amer.Soc.for metals), 9th edition.

Jayaraman N, Ramnath V, 1989. Characterization and wear performance of plasma sprayed WC–Co coatings, *Mater. Sci. Technol.* 5 pp 382–388.

Ji G-C, Wang Y, Li W, 2006. *Surface Coating Technology*; vol. 200,pp 6749.

Kamal.S, Jayaganthan.R, Parkas.S, Kumar S, 2008. Hot corrosion behaviour of detonation gun sprayed Cr_3C_2–NiCr coatings on Ni and Fe-based super alloys in Na2SO4–60% V2O5 environment at 900 °C. *J. Alloys Compd*.; vol.463; pp 358–372.

Li X. M, Yang YY, 1997. Impact wear performances of Cr_3C_2-NiCr coatings by plasma and HVOF spraying, *Wear*, vol. 202, pp 208-214.

Mohanty M. Smith R W, 1996. Sliding wear behaviour of thermally sprayed 75/25 Cr_3C_2/NiCr wear resistant coatings, *Wear* vol.198, pp 251-266.

Murthy JKN , Venkataraman B, 2006. *Surface coating Technology*; volume 200,pp 2642

Murthy JKN, Bysakh S, Gopinath K, Venkataraman B, 2007. *Surface coating Technology*;202:1

Rastegar F Richardson DE, 1997.Alternative to chrome: HVOF cermets coatings for high horse power diesel engines. *Surface coatings Technology*, vol. 90:pp 156-163.

Sidhu T S, Sidhu B S, Prakash.S, 2006. Mechanical and micro structural properties of HVOF sprayed WC–Co and Cr_3C_2-NiCr coatings on the boiler tube steels using LPG as the fuel gas. *J. Mater. Process. Technol*.; vol.171; pp 77–82.

Wang B, 1996. "Erosion-corrosion of thermal sprayed coatings in FBC boilers", *Wear* vol. 199, pp 24-32.